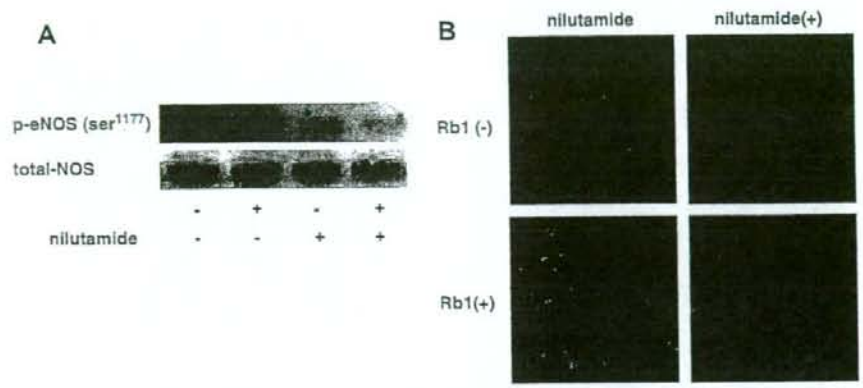

Fig. 4. Effects of nilutamide, an antagonist of androgen receptor, on eNOS phosphorylation and NO production. HAECs were starved 6 h and then treated without or with Rb1 (1 μmol/L) for 30 min. Some groups of cells were pre-treated with androgen receptor agonist nilutamide (10 μmol/L) for 1 h. Cell lysates were then subjected to immunoblotting as described in Materials and methods. The experiments were repeated three times in triplicates, with equal results. Starved cells were loaded with DAF-2 DA as described in Materials and methods before treatment with Rb1 (1 μmol/L). In some groups of cells, nilutamide (10 μmol/L) were added 60 min before cells were loaded with DAF-2 DA. After Rb1 treatment, cells were fixed in 2% paraformaldehyde for 10 min at 4 °C and then viewed using a fluorescent microscope (B). Emission of green light (510 nm) from cells excited by light at 488 nm is indicative of NO production. The experiments were repeated independently three times with equal results. (For interpretation of the references to color in this figure legend, the reader is referred to the web version of this paper.)

Rb1-induced eNOS phosphorylation is inhibited by androgen receptor antagonist

Increasing evidence shows that activation of the steroid hormone receptor such as estrogen receptor (ER) lead to NO production and vasodilation within minutes by non-transcriptional pathways. Ginsenosides have steroidal skeleton structure and can act as an agonist for steroid hormones receptor. To see whether steroid hormone receptors were involved in acute activation of eNOS to produce NO in HUACs by Rb1, we examined the effects of the androgen receptor antagonist nilutamide and estrogen receptor antagonist ICI182780. Representative western blots obtained using anti-phospho-eNOS (Ser1177) antibody and anti-eNOS antibody are shown in Fig. 4A. The Rb1-induced eNOS phosphorylation (Ser1177) was inhibited by the androgen receptor antagonist nilutamid (10 μmol/L) In addition, NO production was diminished to the baseline level in the presence of nilutamid (Fig. 4B). However, the Rb1-induced eNOS phosphorylation (Ser1177) and NO production were unaffected by an estrogen receptor (ER) antagonist ICI182780 (10 μmol/L) (data not shown).

Discussion

We have shown that purified Rb1 rapidly stimulates production of NO in HAECs > 15 min after treatment. Maximal stimulation of NO production was obtained at 30 min. The increase in NO production was abrogated by the addition of eNOS inhibitor, L-NAME. It is generally well known that eNOS is tightly regulated not only at the transcriptional level but also by several post-transcriptional mechanisms [8]. The enhanced phosphorylation at Ser1177 leads to increased eNOS activity. In our experiments, Rb1 induced rapid phosphorylation of eNOS at Ser1177 > 10 min after Rb1 treatment. Maximal eNOS phosphorylation by Rb1 was observed from 30 to 60 min of incubation. NOS activity was also increased by the addition of Rb1 in HAECs. Taken together, our results suggest that the acute effect on NO production in HAECs is attributable to rapid phosphorylation of eNOS at Ser1177. NO produced by eNOS is a fundamental determinant of cardiovascular homeostasis responsible for regulating systolic blood pressure, vascular remodeling and angiogenesis. It is possible to consider that Rb1, a major active component of ginseng could be a candidate responsible for the antihypertensive effects of ginseng previously reported [1,2].

Recent studies have revealed that PI3-kinase/Akt and MEK/ERK1/2 pathways are crucial regulator in cell proliferation, cell-cycle progression, and mediator of cellular survival. Both of them also contribute to enhanced phosphorylation of eNOS at Ser1177/1179 and production of NO [6,7]. The present study showed that Rb1 also stimulated the phosphorylation of Akt (Ser473) and ERK1/2 (Thr202/Thr204) in HAECs. Rb1-induced eNOS phosphorylation was prevented by inhibitors for PI3-kinase/Akt or MEK (ERK kinase). Our data suggest that the activation of PI3-kinase/Akt and MEK/ERK-mediated pathways are involved in the regulation of acute eNOS phosphorylation by ginsenoside Rb1 in HAECs.

Another interesting finding is that acute phosphorylation of eNOS by Rb1 was abolished by an antagonist for androgen receptor. Recent studies have shown Rb1 acts as a phytoestrogen in MCF-7 human mammary carcinoma

cells [9]. However, in HAECs, Rb1-induced eNOS phosphorylation was not prevented by an antagonist for estrogen receptor (data not shown). It is known that testosterone prevents coronary artery disease, and lower testosterone level is a risk factor for ischemic heart disease in men [10–12]. Recent studies revealed that endothelial NO has antiatherosclerotic properties, such as inhibition of platelet aggregation, leukocyte adhesion, smooth muscle cell proliferation, and expression of genes involved in atherosclerosis [4]. Together with these observations, our results that Rb1 induced eNOS phosphorylation has been abolished by the androgen receptor antagonist will be the beginning of the experimental analyses at cellular levels and may provide a clue for better understanding of the mechanisms by which androgens exert their action for preventing coronary artery disease. Further studies are required for elucidation.

Acknowledgments

We thank Drs. K. Yamamoto, K. Hasegawa, Y. Iwaoka, and S. Takasugi for their helpful advices and continuous encouragement.

References

[1] K.H. Han, S.C. Choe, H.S. Kim, D.W. Sohn, K.Y. Nam, B.H. Oh, M.M. Lee, Y.B. Park, Y.S. Choi, J.D. Seo, Y.W. Lee, Effect of red ginseng on blood pressure in patients with essential hypertension and white coat hypertension, Am. J. Chin. Med. 26 (1998) 199–209.

[2] N.D. Kim, S.Y. Kang, V.B. Schini, Ginsenosides evoke endothelium-dependant vascular relaxation in rat aorta, Gen. Pharmacol. 25 (1994) 1071–1077.

[3] N.D. Kim, S.Y. Kang, J.H. Park, V.B. Schini-Kerth, Ginsenoside Rg3 mediates endothelium-dependent relaxation in response to ginsenosides in rat aorta: role of K^+ channels, Eur. J. Pharmacol. 367 (1999) 41–49.

[4] A.G. Herman, S. Moncada, Therapeutic potential of nitric oxide donors in the prevention and treatment of atherosclerosis, Eur. Heart J. 26 (2005) 1945–1955.

[5] H. Kojima, N. Nakatsubo, K. Kikuchi, S. Kawahara, Y. Kirino, H. Nagoshi, Y. Hirata, T. Nagano, Detection and imaging of nitric oxide with novel fluorescent indicators: diaminofluoresceins, Anal. Chem. 70 (1998) 2446–2453.

[6] X. Peng, S. Haldar, S. Deshpande, K. Irani, D.A. Kass, Wall stiffness suppresses Akt/eNOS and cytoprotection in pulse-perfused endothelium, Hypertension 41 (2003) 378–381.

[7] D. Feliers, X. Chen, N. Akis, G.G. Choudhury, M. Madaio, B.S. Kasinath, VEGF regulation of endothelial nitric oxide synthase in glomerular endothelial cells, Kidney Int. 68 (2005) 1648–1659.

[8] I. Fleming, R. Busse, Molecular mechanisms involved in the regulation of the endothelial nitric oxide synthase, Am. J. Physiol. Regul. Integr. Comp. Physiol. 284 (2003) R1–R12.

[9] J. Cho, W. Park, S. Lee, W. Ahn, Y. Lee, Ginsenoside-Rb1 from Panax ginseng C.A. Meyer activates estrogen receptor-alpha and -beta, independent of ligand binding, J. Clin. Endocrinol. Metab. 89 (2004) 3510–3515.

[10] G.B. Phillips, B.H. Pinkernell, T.Y. Jing, The association of hypotesteronemia with coronary artery disease in men, Arterioscler. Thromb. 14 (1994) 701–706.

[11] C.M. Webb, J.G. McNeill, C.S. Hayward, D. De Zeigler, P. Collins, Effects of testosterone on coronary vasomotor regulation in men with coronary heart disease, Circulation 100 (1999) 1690–1696.

[12] F.C. Wu, A. von Eckardstein, Androgens and coronary artery disease, Endocr. Rev. 24 (2003) 183–217.

Available online at www.sciencedirect.com
ScienceDirect
European Journal of Pharmacology 556 (2007) 1–8
www.elsevier.com/locate/ejphar

Gas6/Axl-PI3K/Akt pathway plays a central role in the effect of statins on inorganic phosphate-induced calcification of vascular smooth muscle cells

Bo-Kyung Son [a], Koichi Kozaki [b], Katsuya Iijima [a], Masato Eto [a], Toru Nakano [c], Masahiro Akishita [a], Yasuyoshi Ouchi [a,*]

[a] *Department of Geriatric Medicine, Graduate School of Medicine, The University of Tokyo, 7-3-1 Hongo, Bunkyo-ku, Tokyo 113-8655, Japan*
[b] *Department of Geriatric Medicine, Kyorin University School of Medicine, Tokyo, Japan*
[c] *Discovery Research Laboratory, Shionogi and Co., Ltd., Osaka, Japan*

Received 19 May 2006; received in revised form 22 September 2006; accepted 27 September 2006
Available online 18 October 2006

Abstract

Apoptosis is essential for the initiation and progression of vascular calcification. Recently, we showed that *3-hydroxy-3-methylglutaryl* (HMG) CoA reductase inhibitors (statins) have a protective effect against vascular smooth muscle cell calcification by inhibiting apoptosis, where growth arrest-specific gene 6 (Gas6) plays a pivotal role. In the present study, we clarified the downstream targets of Gas6-mediated survival signaling in inorganic phosphate (Pi)-induced apoptosis and examined the effect of statins. We found that fluvastatin and pravastatin significantly inhibited Pi-induced apoptosis and calcification in a concentration-dependent manner in human aortic smooth muscle cells (HASMC), as was found with atorvastatin previously. Gas6 and its receptor, Axl, expression were downregulated in the presence of Pi, and recombinant human Gas6 (rhGas6) significantly inhibited apoptosis and calcification in a concentration-dependent manner. During apoptosis, Pi suppressed Akt phosphorylation, which was reversed by rhGas6. Wortmannin, a specific *phosphatidylinositol 3-OH kinase* (PI3K) inhibitor, abolished the increase in Akt phosphorylation by rhGas6 and eliminated the inhibitory effect of rhGas6 on both Pi-induced apoptosis and calcification, suggesting that PI3K-Akt is a downstream signal of the Gas6-mediated survival pathway. Pi reduced phosphorylation of Bcl2 and Bad, and activated caspase 3, all of which were reversed by rhGas6. The inhibitory effect of statins on Pi-induced apoptosis was accompanied by restoration of the Gas6-mediated survival signal pathway: upregulation of Gas6 and Axl expression, increased phosphorylation of Akt and Bcl2, and inhibition of Bad and caspase 3 activation. These findings indicate that the Gas6-mediated survival pathway is the target of statins' effect to prevent vascular calcification.

Keywords: Calcification; Apoptosis; Gas6; Axl; Akt; Bcl2

1. Introduction

Vascular calcification, such as coronary and aortic calcification, is clinically important in the development of cardiovascular disease (Eggen, 1968). Two distinct forms of vascular calcification are well recognized. One is medial calcification, which occurs between the cell layers of smooth muscle cells and is related to aging, diabetes and chronic renal failure (Neubauer, 1971; Goodman et al., 2000). The other is atherosclerotic calcification, which occurs in the intima during the development of atheromatous disease (Wexler et al., 1996). In diabetic patients, medial calcification has been shown to be a strong independent predictor of cardiovascular mortality (Everhart et al., 1988).

We recently demonstrated that atorvastatin prevented inorganic phosphate (Pi)-induced calcification by inhibiting apoptosis, one of the important processes regulating calcification. This was mediated by growth arrest-specific gene 6 (Gas6), a vitamin K-dependent protein (Son et al., 2006). Gas6 binds to Axl, the predominant receptor for Gas6, on the cell surface and transduces the signal by Axl autophosphorylation (Mark et al., 1996). Gas6-Axl interaction has been shown to be implicated in the regulation of multiple cellular functions (Yanagita et al., 2001; Goruppi et al., 1996; Nakano et al., 1997; Fridell et al., 1998). Especially, they are known to protect a range of cell types

* Corresponding author. Tel.: +81 3 5800 8652; fax: +81 3 5800 6530.
E-mail address: youchi-tky@umin.ac.jp (Y. Ouchi).

0014-2999/$ - see front matter © 2006 Elsevier B.V. All rights reserved.
doi:10.1016/j.ejphar.2006.09.070

from apoptotic death (Goruppi et al., 1996, 1999; Healy et al., 2001). However, the downstream targets of Gas6-mediated signaling in Pi-induced apoptosis and the effect of statins on this pathway are poorly understood.

With respect to the targets of Gas6-Axl interaction, Lee et al. (2002) showed that activation of Akt is necessary for Gas6-dependent cell survival. Akt is an important mediator of metabolic and survival responses after growth factor stimulation. Akt is activated by phosphorylation, which is performed by phosphatidylinositol 3-OH kinase (PI3K), a kinase that is activated by Gas6-Axl interaction (Lee et al., 2002; Ming Cao et al., 2001). Activation of Akt leads to downstream signaling events including those associated with mitochondrial regulators of apoptosis such as Bcl2 and Bad.

In the present study, we examined the effect of statins using two different types: lipophilic fluvastatin and hydrophilic pravastatin. We investigated the effect of statins on Pi-induced apoptosis and calcification as well as on signaling components in this process. Consequently, we found that both statins restored the Gas6-mediated survival pathway, with upregulation of the expression of Gas6 and Axl, increased phosphorylation of Akt, Bcl2 and Bad; and finally inhibition of caspase 3 activation, resulting in the prevention of apoptosis and subsequent calcification in human aortic smooth muscle cells (HASMC).

2. Materials and methods

2.1. Materials

Pravastatin and fluvastatin were supplied by Sankyo Co. Ltd. and Tanabe Seiyaku Co., Ltd., respectively. Recombinant human Gas6 (rhGas6) was prepared as described previously (Ming et al., 2001). Wortmannin was purchased from Calbiochem. All other reagents were of analytical grade.

2.2. Cell culture

HASMC were obtained from Clonetics. They were cultured in Dulbecco's modified Eagle's medium (DMEM) supplemented with 20% *fetal bovine serum* (FBS), 100 U/ml penicillin and 100 mg/ml streptomycin at 37 °C in a humidified atmosphere with 5% CO_2. HASMC were used up to passage 8 for the experiments.

2.3. Induction and quantification of calcification

For Pi-induced calcification, Pi (a mixed solution of Na_2HPO_4 and NaH_2PO_4 whose pH was adjusted to 7.4) was added to serum-supplemented DMEM to a final concentration of 2.6 mM. After the indicated incubation period, cells were decalcified with 0.6 M HCl, and Ca content in the supernatant was determined by the *o*-cresolphthalein complexone method (C-Test, WAKO). The remaining cells were solubilized in 0.1 M NaOH/0.1% *sodium dodecyl sulfate* (SDS), and cell protein content was measured by Bio-Rad protein assay. Calcification was visualized by von Kossa's method. Briefly, the cells were fixed with 4% formaldehyde and exposed to 5% aqueous $AgNO_3$.

2.4. Induction and determination of apoptosis

Two different time courses were tested to investigate Pi-induced apoptosis and examine the effect of statins, under short-term (within 24 h) and long-term (up to 10 days) conditions (Son et al., 2006).

2.4.1. TdT-mediated dUTP nick end-labeling (TUNEL) assay

TUNEL assay to detect DNA fragmentation was performed using a commercially available kit (ApopTag Plus, Chemicon). Briefly, the samples were preincubated with equilibration buffer for 10 min, and subsequently incubated with terminal deoxyribonucleotidyl transferase in the presence of digoxigenin-conjugated dUTP for 1 h at 37 °C. The reaction was terminated by incubating the samples in stopping buffer for 30 min. After 3 rinses with *phosphate-buffered saline* (PBS), a fluorescein-labeled anti-digoxigenin antibody was applied for 30 min, and the samples were rinsed 4 times with PBS. The samples were then stained, mounted with DAPI (*4′,6-diamino-2-phenylindole*)/antifade, and examined by fluorescence microscopy.

2.4.2. Detection of DNA fragmentation by ELISA

Cytoplasmic histone-associated DNA fragments were determined with a cell-death detection ELISA^{plus} kit (Roche) as a quantitative index of apoptosis. Briefly, after the cells were incubated in lysis buffer for 30 min, 20 μl of the cell lysates was used for the assay. Following addition of substrate, colorimetric change was determined as the absorbance value measured at 405 nm.

2.5. Immunoblotting

The effect of Pi and statins on the expression of Gas6 and Axl, phosphorylation of Akt, Bcl2 and Bad, and activation of caspase 3 was examined at 12 h. The collected cell lysates were applied to SDS-polyacrylamide gels under reducing conditions, and transferred to a polyvinylidene difluoride (PVDF) membrane. Immunoblot analysis was performed using specific primary antibodies: anti-Axl, anti-Gas6 (Santa Cruz Biotechnology), anti-caspase 3, anti-Akt, anti-Bcl2, anti-phospho-Akt, anti-phospho-Bcl2, anti-phospho-Bad (Cell Signaling Technology), and anti-Bad (Transduction Laboratories). After incubation with horseradish peroxidase-conjugated secondary antibodies (Amersham Pharmacia), blots were visualized by enhanced chemiluminescence and autoradiography (ECL Plus, Amersham Pharmacia). Experiments were performed with at least three different cell populations.

2.6. Statistical analysis

All results are presented as mean±S.E.M. Statistical comparisons were made by ANOVA, unless otherwise stated. A value of $P<0.05$ was considered to be significant.

3. Results

3.1. Statins inhibit Pi-induced apoptosis and calcification in HASMC

In HASMC, a high Pi level (≥2.6 mM), comparable to that of hyperphosphatemia in end-stage renal disease, significantly induced calcification. Fluvastatin showed an inhibitory effect on Pi-induced calcification at as high a concentration as 0.1 μM (26.1±2.3% of control), while pravastatin showed the degree of effect at 50 μM (27.4±3.1% of control) (Fig. 1A). An inhibitory effect on Ca deposition was also found by von Kossa's staining (Fig. 1B). Both statins prevented Pi-induced apoptosis at the same concentrations as those at which they prevented calcification (Fig. 1C). An antiapoptotic effect of statins was also observed by TUNEL assay on day 6 (Fig. 1D).

3.2. Gas6 plays an important role in Pi-induced apoptosis

In the presence of 2.6 mM Pi, the expression of Gas6 and Axl was markedly downregulated (Fig. 2A). To investigate the role of Gas6 in Pi-induced apoptosis and calcification, first, we tested whether supplementation of rhGas6 could prevent Pi-induced apoptosis. In HASMC, rhGas6 significantly inhibited Pi-induced apoptosis in a concentration-dependent manner (Fig. 2B). Furthermore, during apoptosis, activated products of caspase 3 (17 and 19 kDa) were significantly increased by 2.6 mM Pi, which was reversed by rhGas6 (Fig. 2C). Next, we examined the effect of rhGas6 on calcification. Recombinant human Gas6 significantly inhibited Pi-induced calcification on day 6 in a concentration-dependent manner (Fig. 2D), suggesting that Gas6 plays an important role in Pi-induced apoptosis and calcification.

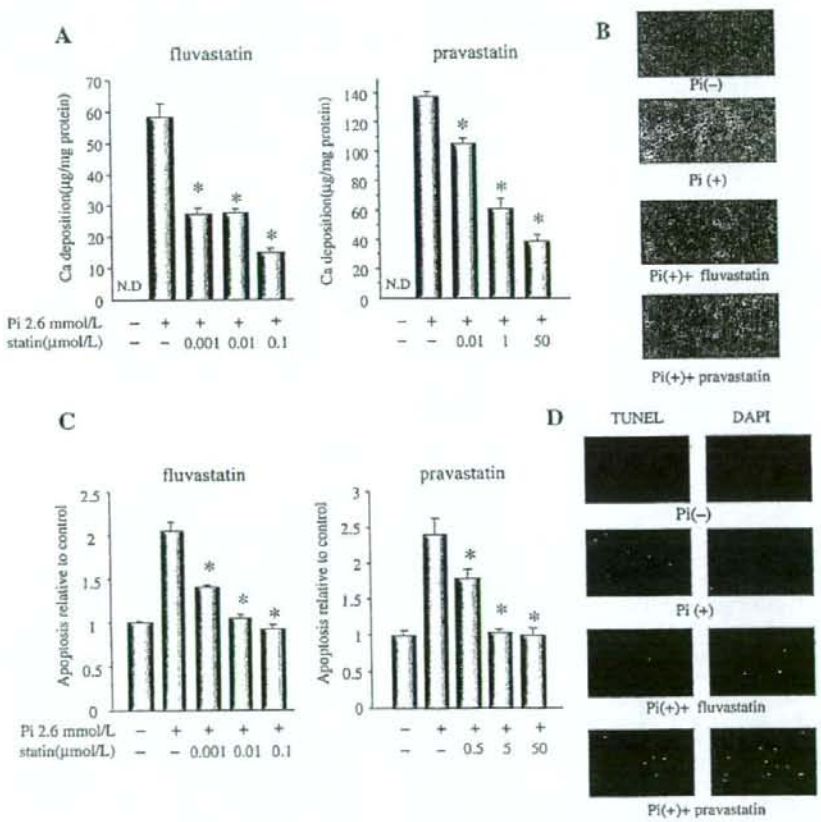

Fig. 1. Statins prevent Pi-induced apoptosis and calcification. HASMC were cultured with the indicated concentrations of fluvastatin and pravastatin in the presence of 2.6 mM Pi for 6 days. Ca deposition was measured by *o*-cresolphthalein complexone method, and normalized by cell protein content. All values are presented as mean± S.E.M. ($n=6$). *$P<0.05$ vs. statin (−) by Fisher's test. N.D. stands for "not detected" (A). On day 6, the inhibitory effect of fluvastatin (0.1 μM) and pravastatin (50 μM) on 2.6 mM Pi [Pi(+)]-induced Ca deposition was evaluated at the light microscopic level with von Kossa's staining (B). Serum-starved HASMC were cultured with the indicated concentrations of fluvastatin and pravastatin for 12 h and then incubated with 2.6 mM Pi for an additional 24 h. A quantitative index of apoptosis, determined by ELISA, is presented as the relative value to that without statins and 2.6 mM Pi. All values are presented as mean±S.E.M. ($n=3$). *$P<0.05$ vs. 2.6 mM Pi, statin (−) by Fisher's test (C). The antiapoptotic effect of fluvastatin (0.1 μM) and pravastatin (50 μM) was evaluated by TUNEL staining (green) on day 6. Nuclei were counterstained with DAPI (4′,6-diamino-2-phenylindole, blue) (D).

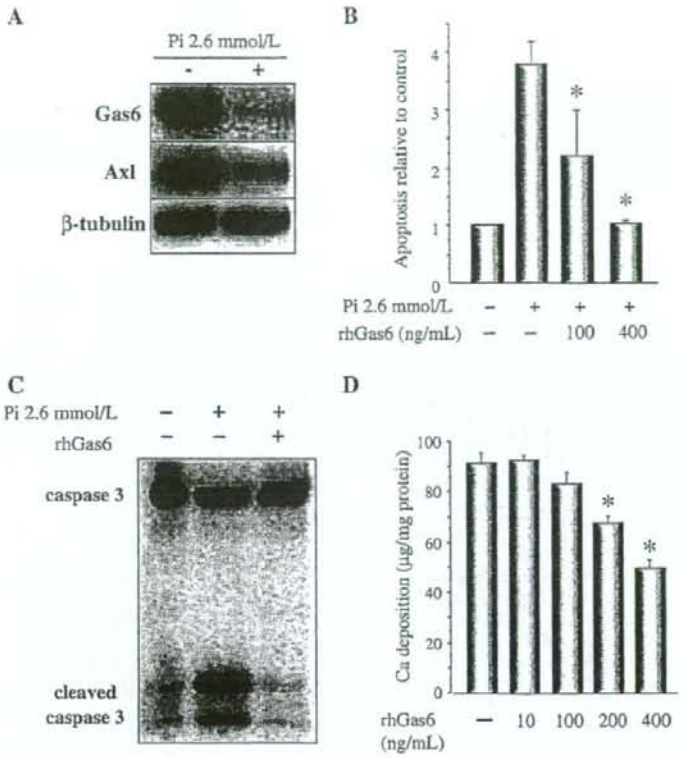

Fig. 2. Pi suppresses Gas6 and Axl expression, and rhGas6 inhibits caspase-dependent apoptosis and calcification. HASMC were cultured in the presence or absence of 2.6 mM Pi for 12 h. Cell lysates were collected and subjected to SDS-PAGE followed by immunoblotting with antibodies to Gas6, Axl or β-tubulin (A). After pretreatment with the indicated concentrations of rhGas6, apoptosis was induced by 2.6 mM Pi. All values are presented as mean±S.E.M. ($n=3$). *$P<0.05$ vs. 2.6 mM Pi, rhGas6 (−) by Fisher's test (B). HASMC were pretreated with rhGas6 (400 ng/ml) for 1 h, then cultured with 2.6 mM Pi for 12 h. Cell lysates were immunoblotted with an antibody that recognizes caspase-3 (35 kDa) and the cleaved forms of caspase-3 (17 and 19 kDa) (C). For measurement of Ca deposition, HASMC were cultured with the indicated concentrations of rhGas6 in the presence of 2.6 mM Pi for 6 days. All values are presented as mean±S.E.M. ($n=6$). *$P<0.05$ by Fisher's test (D). Experiments were performed with at least three different cell populations.

3.3. Downregulation of phospho-Akt participates in Pi-induced apoptosis

Since in NIH-3T3 fibroblasts, the antiapoptotic effect of Gas6-Axl interaction has been shown to be mediated by Akt phosphorylation (Goruppi et al., 1999), we examined whether Akt participates in the signaling of downregulation of the Gas6-Axl interaction during Pi-induced apoptosis. In the presence of 2.6 mM Pi, Akt phosphorylation was downregulated in a time-dependent manner, whereas the expression of total Akt was not changed (Fig. 3A). In addition, rhGas6 abrogated the Pi-induced decrease in Akt phosphorylation, implying that subsequent downregulation of Akt phosphorylation is the pathway of Pi-induced apoptosis (Fig. 3B).

Because Akt phosphorylation is regulated by PI3K, we examined the effect of wortmannin, a specific PI3K inhibitor, on rhGas6-mediated phosphorylation of Akt. As shown in Fig. 3B, wortmannin abrogated the rhGas6-induced phosphorylation of Akt and further eliminated the inhibitory effect of rhGas6 on Pi-induced apoptosis and calcification (Fig. 3C, D). These results indicate that the preventive effect of rhGas6 on Pi-induced apoptosis and calcification was mediated by the PI3K-Akt pathway.

3.4. Pi suppresses Bcl2 phosphorylation and activates Bad

To establish the downstream components of Pi-induced apoptosis, two key apoptosis-regulating proteins, Bcl2 and Bad, were analyzed. During apoptosis, phosphorylation of Bcl2 (active form) and Bad (inactive form) was markedly reduced by 2.6 mM Pi in a time-dependent manner. The expression level of their total protein was not changed in this period (Fig. 4A, B). By supplementation of the medium with rhGas6, the decrease in phosphorylation of Bcl2 and Bad by Pi was reversed to almost the basal level (Fig. 4C, D). These results indicate that Pi promotes apoptosis by inactivating Bcl2 and activating Bad via a Gas6-dependent pathway.

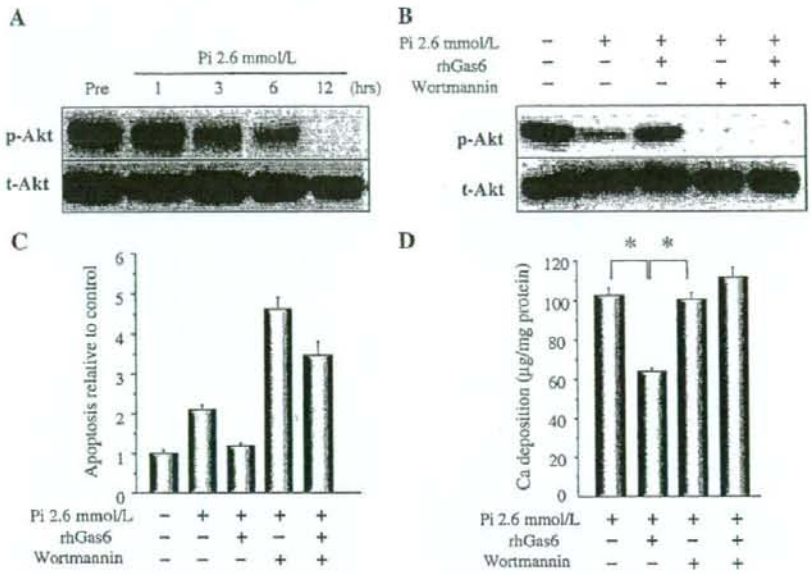

Fig. 3. Pi decreases Akt phosphorylation, and wortmannin abrogates the inhibitory effect of rhGas6 on Akt phosphorylation, apoptosis and calcification. HASMC were cultured in the presence of 2.6 mM Pi for the indicated periods. Cell lysates were immunoblotted with anti-phospho-Akt (p-Akt) antibody and total Akt (t-Akt) antibody (A). HASMC were pretreated with rhGas6 (400 ng/ml), wortmannin (1 μM), or both for 1 h, and then treated with 2.6 mM Pi for 12 h. Cell lysates were immunoblotted with p-Akt and t-Akt antibody (B). After pretreatment with rhGas6 (400 ng/ml) and wortmannin (1 μM), apoptosis was induced by 2.6 mM Pi. All values are presented as mean±S.E.M. ($n=3$). $^*P<0.05$ vs. 2.6 mM Pi, rhGas6 (−), wortmannin (−) by Fisher's test (C). HASMC were cultured with rhGas6 (400 ng/ml) and with or without wortmannin (1 μM) in the presence of 2.6 mM Pi for 6 days. Ca content was measured and normalized by cell protein content. All values are presented as mean±S.E.M. ($n=6$). $^*P<0.05$ by Fisher's test (D).

3.5. Gas6-mediated survival pathway is the target of statins' effect on apoptosis

To investigate whether the antiapoptotic effect of statins is associated with the Gas6-mediated survival pathway, first, we examined the effect of statins on the expression of Gas6 and Axl. As shown in Fig. 5A and B, both fluvastatin and pravastatin restored the expression of Gas6 and Axl, which was downregulated by 2.6 mM Pi. Because we have shown that the Gas6-mediated survival pathway is Akt-dependent, the effect of statins on Akt phosphorylation was examined. The Pi-induced decrease in Akt phosphorylation was restored by both statins, while total Akt expression was not changed. In addition, we found that both statins stimulated phosphorylation of Bcl2 and

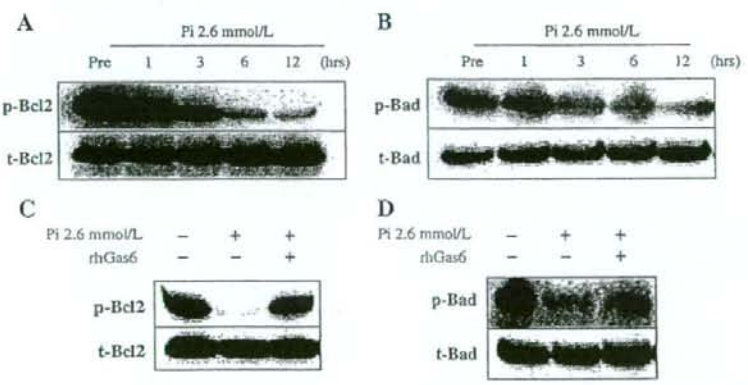

Fig. 4. RhGas6 restores Pi-induced decrease in phosphorylation of Bcl2 and Bad. HASMC were exposed to 2.6 mM Pi for the indicated periods, and cell lysates were subjected to immunoblotting with anti-phospho-Bcl2 (p-Bcl2) antibody and total Bcl2 (t-Bcl2) antibody (A), or with anti-phospho-Bad (p-Bad) antibody and total Bad (t-Bad) antibody (B). HASMC were pretreated with rhGas6 (400 ng/ml) for 1 h, and then treated with 2.6 mM Pi for 12 h. Cell lysates were subjected to immunoblotting with p-Bcl2 and t-Bcl2 antibody (C), or with p-Bad and t-Bad antibody (D).

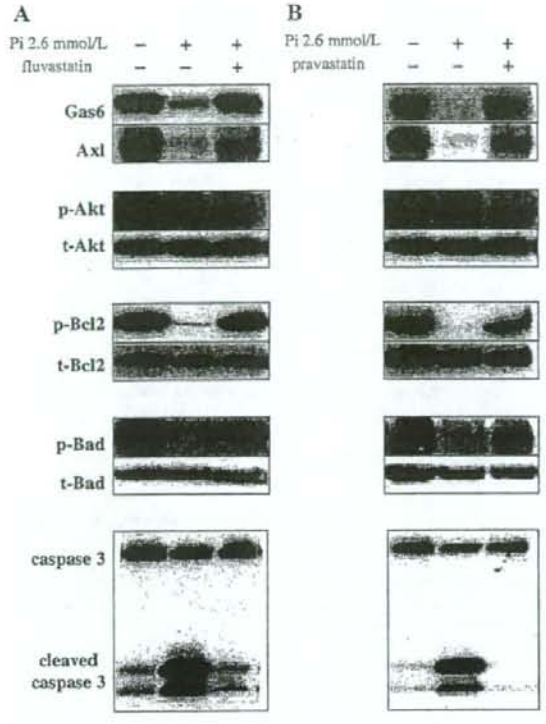

Fig. 5. Antiapoptotic effect of statins is associated with upregulation of Gas6-Axl survival pathway. After pretreatment with 0.1 μM fluvastatin (A) and 50 μM pravastatin (B) for 12 h, apoptosis was induced by 2.6 mM Pi. After 12 h, cell lysates were collected and subjected to SDS-PAGE followed by immunoblotting with antibodies that recognize Gas6 and Axl, with phospho-specific Akt (p-Akt) and total Akt (t-Akt) antibody, with phospho-specific Bcl2 (p-Bcl2) and total Bcl2 (t-Bcl2) antibody, or with phospho-specific Bad (p-Bad) and total Bad (t-Bad) antibody. Cell lysates were immunoblotted with an antibody that recognizes uncleaved caspase-3 (35 kDa) and the cleaved forms of caspase-3 (17 and 19 kDa).

Bad, with total expression unchanged. Pi-induced caspase 3 activation was also prevented by both statins. Taken together, these findings suggest that the inhibitory effect of statins on Pi-induced apoptosis is mediated by restoration of the Gas6-mediated survival pathway; PI3K-induced Akt phosphorylation, Bcl2 activation, Bad inactivation, and caspase 3 inactivation.

4. Discussion

In the present study, we found that both lipophilic fluvastatin and hydrophilic pravastatin protected against Pi-induced apoptosis and calcification in HASMC, as we found with atorvastatin previously. With regard to the different potency of statins, we found that the inhibitory effect of pravastatin was inferior to those of fluvastatin and atorvastatin, which exerted similar effects on calcification and apoptosis. This might relate to our previous finding that the inhibition of calcification by statins was not dependent on the mevalonate pathway (Son et al., 2006). Consequently, the inhibitory effect on calcification was not parallel to the cholesterol-lowering effect. We speculate that the difference between statins was derived from their affinity to *vascular smooth muscle cells* (VSMC), that is, lipophilic statins have stronger effects on VSMC calcification than hydrophilic statins.

The antiapoptotic effect of statins was induced by restoration of the Gas6-mediated survival pathway: PI3K-induced Akt phosphorylation, Bcl2 and Bad phosphorylation, and caspase 3 inactivation. Gas6 plays a crucial role in the effect of statins on Pi-induced apoptosis. Gas6, a secreted vitamin K-dependent protein, binds to the receptors of the mammalian Axl protein-tyrosine kinase family; Axl, Sky, and Mer, with different affinities (Nagata et al., 1996). Gas6 and Axl have been shown to localize in the neointima of the artery after balloon injury, in which they presumably modulate several cell functions such as differentiation, adhesion, migration, proliferation, and survival in a cell-specific manner (Melaragno et al., 1998). The Gas6-Axl interaction is also shown to upregulate scavenger receptor A expression in VSMC (Ming et al., 2001), and facilitates the clearance of apoptotic cells by macrophages (Ishimoto et al., 2000). Of the above functions, protection against apoptotic cell death has been most studied (Goruppi et al., 1996; Healy et al., 2001; Lee et al., 2002; Nakano et al., 1996). Consistently, the expression of Gas6 and Axl was downregulated by Pi, leading to apoptosis and subsequent calcification.

Several intracellular signaling pathways mediated by Gas6-Axl interaction have been shown previously (Goruppi et al., 1999; Lee et al., 2002; Ming et al., 2001). Akt, which is necessary for Gas6-dependent survival, is a critical downstream effector of the PI3K-dependent antiapoptotic pathway. In VSMC, it has been reported that the PI3K-Akt pathway mediates Gas6 induction of scavenger receptor A (Ming et al., 2001). Consistent with these reports, our study provides evidence that the PI3K-Akt pathway is a target of Gas6-Axl interaction, and downregulation of Akt phosphorylation is associated with Pi-induced apoptosis and calcification. Moreover, it is known that PI3K-Akt affects the cell death program through the Bcl2 family of proteins. This protein family is a critical regulator of apoptosis in a variety of cell types, and the balance of antiapoptotic members, such as Bcl2, versus proapoptotic mediators, such as Bad, determines cell fate (Reed, 1997). Bcl2, whose phosphorylation is required for its antiapoptotic activity (Ruvolo et al., 2001), inhibits programmed cell death by several mechanisms: It binds to caspase CED-4 (Apaf-1) and prevents the cell execution cascade; Bcl2 alters mitochondrial membrane potential and inhibits the release of cytochrome c. On the other hand, Bad plays a proapoptotic role in its dephosphorylated form by binding to Bcl2 and reversing its antiapoptotic effect; phosphorylation of Bad results in its cytosolic sequestration by 14-3-3 and hampers its binding to Bcl2 (Zha et al., 1996). It was also reported that Bad is directly phosphorylated by PI3K-Akt (del Peso et al., 1997). In the present study, Bcl2 was inactivated and Bad was activated (both proteins were dephosphorylated) by Pi, directing the cells to apoptosis, and rhGas6 restored phosphorylation of Bcl2 and Bad. During apoptosis, one of the final biochemical events leading to programmed

cell death is activation of the caspase cascade. Activation of caspase 3 is required for internucleosomal DNA degradation (Woo et al., 1998), and caspase inhibition prevents the release of apoptotic bodies from cells (Zhang et al., 1999). In the present study, supplementation of the medium with rhGas6 prevented Pi-induced caspase 3 activation. These results clearly show that Pi downregulates Gas6-Axl, decreases PI3K-mediated Akt phosphorylation, inactivates Bcl2, activates Bad, and activates caspase 3, leading to apoptosis.

The present study demonstrated that statins restored the Gas6-mediated survival pathway. Consistent with these results, Akt phosphorylation has been reported to be an antiapoptotic mechanism of statins: pravastatin inhibited hypoxia-induced apoptosis through activation of Akt in cardiomyocytes (Bergmann et al., 2004), and simvastatin and pravastatin enhanced phosphorylation of Akt and promoted angiogenesis in endothelial cells (Kureishi et al., 2000). Recently, it was reported that statins inhibit caspase 3 activation driven by protein kinase C inhibitors in the process of apoptosis, suggesting that caspase 3 is also under the control of statins during apoptosis (Tanaka et al., 2004).

In this study, we performed experiments under both short-term (within 24 h) and long-term (up to 10 days) conditions. In general, short-term experiments are able to examine acute cell behavior, such as signaling and transcription. However, because obvious HASMC calcification takes at least 3 days, we also performed long-term experiments. Downregulation of Gas6, Axl expression and reduced phosphorylation of Akt, Bcl2, and Bad, and a beneficial effect of statins were consistently found in the long-term condition. This confirms that the Gas6-Axl survival signal is the key mechanism for Pi-induced calcification.

It is concluded that statins inhibit Pi-induced apoptosis via the Gas6/Axl-PI3K-Akt signal pathway, which has a crucial role in the prevention of HASMC calcification. This study adds further evidence of the pleiotropic effects of statins, suggesting a therapeutic strategy for the prevention of vascular calcification.

Acknowledgements

This study was supported by a Grant-in-Aid for Scientific Research from the Ministry of Education, Science, Sports, and Culture of Japan (No. 15390239), Mitsui Sumitomo Insurance Welfare Foundation, Ono Medical Research Foundation, Kanzawa Medical Research Foundation, Novartis Foundation for Gerontological Research, and Takeda Research Foundation. We thank Yuki Ito for technical assistance.

References

Bergmann, M.W., Rechner, C., Freund, C., Baurand, A., Jamali, A., Dietz, R., 2004. Statins inhibit reoxygenation-induced cardiomyocyte apoptosis: role for glycogen synthase kinase 3β and transcription factor β-catenin. J. Mol. Cell. Cardiol. 37, 681–690.

del Peso, L., Gonzalez-Garcia, M., Page, C., Herrera, R., Nunez, G., 1997. Interleukin-3-induced phosphorylation of Bad through protein kinase Akt. Science 278, 687–689.

Eggen, D.A., 1968. Relationship of calcified lesions to clinically significant atherosclerotic lesions. Ann. N. Y. Acad. Sci. 149, 752–767.

Everhart, J.E., Pettitt, D.J., Knowler, W.C., Rose, F.A., Bennett, P.H., 1988. Medial artery calcification and its association with mortality and complications of diabetes. Diabetologia 31, 16–23.

Fridell, Y.W., Villa Jr., J., Attar, E.C., Liu, E.T., 1998. Gas6 induces Axl-mediated chemotaxis of vascular smooth muscle cells. J. Biol. Chem. 273, 7123–7126.

Goodman, W.G., Goldin, J., Kuizon, B.D., Yoon, C., Gales, B., Sider, D., Wang, Y., Chung, J., Emerick, A., Greaser, L., Elashoff, R.M., Salusky, I.B., 2000. Coronary-artery calcification in young adults with end-stage renal disease who are undergoing dialysis. N. Engl. J. Med. 342, 1478–1483.

Goruppi, S., Ruaro, E., Schneider, C., 1996. Gas6, the ligand of Axl tyrosine kinase receptor, has mitogenic and survival activities for serum starved NIH3T3 fibroblasts. Oncogene 12, 471–480.

Goruppi, S., Ruaro, E., Varnum, B., Schneider, C., 1999. Gas6-mediated survival in NIH3T3 cells activates stress signaling cascade and is independent of Ras. Oncogene 18, 4224–4236.

Healy, A.M., Schwartz, J.J., Zhu, X., Herrick, B.E., Varnum, B., Farber, H.W., 2001. Gas6 promotes Axl-mediated survival in pulmonary endothelial cells. Am. J. Physiol., Lung Cell. Mol. Physiol 280, L1273–L1281.

Ishimoto, Y., Ohashi, K., Mizuno, K., Nakano, T., 2000. Promotion of the uptake of PS liposomes and apoptotic cells by a product of growth arrest-specific gene, gas6. J. Biochem. (Tokyo) 127, 411–417.

Kureishi, Y., Luo, Z., Shiojima, I., Bialik, A., Fulton, D., Lefer, D.J., Sessa, W.C., Walsh, K., 2000. The HMG-CoA reductase inhibitor simvastatin activates the protein kinase Akt and promotes angiogenesis in normocholesterolemic animals. Nat. Med. 6, 1004–1010.

Lee, W.P., Wen, Y., Varnum, B., Hung, M.C., 2002. Akt is required for Axl-Gas6 signaling to protect cells from E1A-mediated apoptosis. Oncogene 21, 329–336.

Mark, M.R., Chen, J., Hammonds, R.G., Sadick, M., Godowsk, P.J., 1996. Characterization of Gas6, a member of the superfamily of G domain-containing proteins, as a ligand for Rse and Axl. J. Biol. Chem. 271, 9785–9789.

Melaragno, M.G., Wuthrich, D.A., Poppa, V., Gill, D., Lindner, V., Berk, B.C., Corson, M.A., 1998. Increased expression of Axl tyrosine kinase after vascular injury and regulation by G protein-coupled receptor agonists in rats. Circ. Res. 83, 697–704.

Ming Cao, W., Murao, K., Imachi, H., Sato, M., Nakano, T., Kodama, T., Sasaguri, Y., Wong, N.C., Takahara, J., Ishida, T., 2001. Phosphatidylinositol 3-OH kinase-Akt/protein kinase B pathway mediates Gas6 induction of scavenger receptor a in immortalized human vascular smooth muscle cell line. Arterioscler. Thromb. Vasc. Biol. 21, 1592–1597.

Nagata, K., Ohashi, K., Nakano, T., Arita, H., Zong, C., Hanafusa, H., Mizuno, K., 1996. Identification of the product of growth arrest-specific gene 6 as a common ligand for Axl, Sky, and Mer receptor tyrosine kinases. J. Biol. Chem. 271, 30022–30027.

Nakano, T., Kawamoto, K., Higashino, K., Arita, H., 1996. Prevention of growth-arrest induced cell death of vascular smooth muscle cells by a product of growth arrest-specific gene, gas6. FEBS Lett. 387, 78–80.

Nakano, T., Ishimoto, Y., Kishino, J., Umeda, M., Inoue, K., Nagata, K., Ohashi, K., Mizuno, K., Arita, H., 1997. Cell adhesion to phosphatidylserine mediated by a product of growth arrest-specific gene 6. J. Biol. Chem. 272, 29411–29414.

Neubauer, B., 1971. A quantitative study of peripheral arterial calcification and glucose tolerance in elderly diabetics and non-diabetics. Diabetologia 7, 409–413.

Reed, J.C., 1997. Double identity for proteins of the Bcl-2 family. Nature 387, 773–776.

Ruvolo, P.P., Deng, X., May, W.S., 2001. Phosphorylation of Bcl2 and regulation of apoptosis. Leukemia 515–522.

Son, B.K., Kozaki, K., Iijima, K., Eto, M., Kojima, T., Ota, H., Senda, Y., Maemura, K., Nakano, T., Akishita, M., Ouchi, Y., 2006. Statins protect human aortic smooth muscle cells from inorganic phosphate-induced calcification by restoring Gas6-Axl survival pathway. Circ. Res. 98, 1024–1031.

Tanaka, K., Honda, M., Takabatake, T., 2004. Anti-apoptotic effect of atorvastatin, a 3-hydroxy-3-methylglutaryl coenzyme a reductase inhibitor, on cardiac myocytes through protein kinase C activation. Clin. Exp. Pharmacol. Physiol. 31, 360–364.

Wexler, L., Brundage, B., Crouse, J., Detrano, R., Fuster, V., Maddahi, J., Rumberger, J., Stanford, W., White, R., Taubert, K., 1996. Coronary artery calcification: pathophysiology, epidemiology, imaging methods, and clinical

implications. A statement for health professionals from the American Heart Association. Writing Group. Circulation 94, 1175–1192.

Woo, M., Hakem, R., Soengas, M.S., Duncan, G.S., Shahinian, A., Kagi, D., Hakem, A., McCurrach, M., Khoo, W., Kaufman, S.A., Senaldi, G., Howard, T., Lowe, S.W., Mak, T.W., 1998. Essential contribution of caspase3/CPP32 to apoptosis and its associated nuclear changes. Genes Dev. 12, 806–819.

Yanagita, M., Arai, H., Ishii, K., Nakano, T., Ohashi, K., Mizuno, K., Vamum, B., Fukatsu, A., Doi, T., Kita, T., 2001. Gas6 regulates mesangial cell proliferation through Axl in experimental glomerulonephritis. Am. J. Pathol. 158, 1423–1432.

Zha, J., Harada, H., Yang, E., Jockel, J., Korsmeyer, S.J., 1996. Serine phosphorylation of death agonist BAD in response to survival factor results in binding to 14-3-3 not BCL-X(L). Cell 87, 619–628.

Zhang, J., Reedy, M.C., Hannun, Y.A., Obeid, L.M., 1999. Inhibition of caspases inhibits the release of apoptotic bodies: Bcl2 inhibits the initiation of formation of apoptotic bodies in chemotherapeutic agent-induced apoptosis. J. Cell Biol. 145, 99–108.

ELSEVIER

Atherosclerosis 191 (2007) 281–289

ATHEROSCLEROSIS

www.elsevier.com/locate/atherosclerosis

Potent free radical scavenger, edaravone, suppresses oxidative stress-induced endothelial damage and early atherosclerosis

Hang Xi[a], Masahiro Akishita[b,*], Kumiko Nagai[a], Wei Yu[a], Hiroshi Hasegawa[a], Masato Eto[b], Koichi Kozaki[a], Kenji Toba[a]

[a] *Department of Geriatric Medicine, Kyorin University School of Medicine, Tokyo, Japan*
[b] *Department of Geriatric Medicine, Graduate School of Medicine, University of Tokyo, 7-3-1 Hongo, Bunkyo-ku, Tokyo 113-8655, Japan*

Received 28 November 2005; received in revised form 9 May 2006; accepted 19 May 2006
Available online 27 June 2006

Abstract

Objective: Effects of potent free radical scavenger, edaravone, on oxidative stress-induced endothelial damage and early atherosclerosis were investigated using animal models and cultured cells.
Methods and results: Endothelial apoptosis was induced by 5-min intra-arterial exposure of a rat carotid artery with 0.01 mmol/L H_2O_2. Edaravone treatment (10 mg/kg i.p.) for 3 days suppressed endothelial apoptosis, as evaluated by chromatin staining of *en face* specimens at 24 h, by approximately 40%. Similarly, edaravone dose-dependently inhibited H_2O_2-induce apoptosis of cultured endothelial cells in parallel with the inhibition of 8-isoprostane formation, 4-hydroxy-2-nonenal (4-HNE) accumulation and VCAM-1 expression. Next, apolipoprotein-E knockout mice were fed a high-cholesterol diet for 4 weeks with edaravone (10 mg/kg i.p.) or vehicle treatment. Edaravone treatment decreased atherosclerotic lesions in the aortic sinus (0.18 ± 0.01 to 0.09 ± 0.01 mm^2, $P < 0.001$) and descending aorta (5.09 ± 0.86 to 1.75 ± 0.41 mm^2, $P < 0.05$), as evaluated by oil red O staining without influence on plasma lipid concentrations or blood pressure. Dihydroethidium labeling and cytochrome *c* reduction assay showed that superoxide anions in the aorta were suppressed by edaravone. Also, plasma 8-isoprostane concentrations and aortic nitrotyrosine, 4-HNE and VCAM-1 contents were decreased by edaravone treatment.
Conclusions: These results suggest that edaravone may be a useful therapeutic tool for early atherosclerosis, pending the clinical efficacy.

Keywords: Atherosclerosis; Reactive oxygen species; Free radical scavenger; Edaravone; 4-HNE; Apolipoprotein E knockout mouse

1. Introduction

Accumulating evidence has shown that stress-induced injury of vascular endothelial cells (ECs) is an initial event in the development of atherosclerosis [1]. In particular, oxidative stress has been implicated in endothelial injury caused by oxidized LDL and smoking as well as hypertension, diabetes and ischemia-reperfusion [1–3]. This notion is supported by the findings that the production of reactive oxygen species (ROS) is upregulated in vascular lesions [4,5], and that lesion formations such as endothelial dysfunction [6] and atherosclerosis [7] are accelerated by superoxide anion ($O_2^{\bullet -}$).

Experimental studies have shown the protective effects of antioxidants on atherosclerosis and endothelial injury. Dietary antioxidants were reported to preserve endothelial function [8,9] and inhibit atherosclerosis [10] in cholesterol-fed rabbits. In a well employed animal model of atherosclerosis, apolipoprotein E knockout (ApoE-KO) mouse fed a high fat diet, it has been shown that there was a significant increase in basal superoxide products [11,12], and that both $O_2^{\bullet -}$ levels and aortic lesion areas were attenuated by treatment with Vitamin E [11] or superoxide dismutase [13]. By contrast, it has been reported that elimination of NAD(P)H oxidase [14] or disruption of its subunit p47phox [15] had no effect on lesion size in ApoE-KO mice. Clinical experiments have

* Corresponding author. Tel.: +81 3 5800 8832; fax: +81 3 5800 8831.
E-mail address: akishita-tky@umin.ac.jp (M. Akishita).

0021-9150/$ – see front matter © 2006 Elsevier Ireland Ltd. All rights reserved.
doi:10.1016/j.atherosclerosis.2006.05.040

also shown that antioxidants such as Vitamins C and E can ameliorate endothelial dysfunction in patients with hypercholesterolemia or atherosclerosis [16,17], although recent clinical trials have failed to prove the protective effects of Vitamin E on cardiovascular events in patients with risk factors [18] and in healthy subjects [19].

Edaravone is a potent free radical scavenger that has been clinically used to reduce the neuronal damage following ischemic stroke [20]. Edaravone has promising property to quench hydroxyl radical (•OH) and show inhibitory effects on peroxynitrite ($ONOO^-$) and both water-soluble and lipid-soluble peroxyl radical ($LOO^•$) [21,22]. Accordingly, this compound exerts a wide range of antioxidant activity on ROS beyond the effects of water-soluble or lipid-soluble antioxidant vitamins. Based on this idea, we hypothesized that edaravone would inhibit the process of atherosclerosis.

To test this hypothesis, we investigated the effects of edaravone in two experimental models. First, we examined whether edaravone could inhibit hydrogen peroxide (H_2O_2)-induced EC apoptosis in a rat model [23] and cultured ECs. Second, we examined whether edaravone could suppress the atherosclerotic lesion formation in ApoE-KO mice.

2. Methods

2.1. Animals

Male Wistar rats aged 10–12 weeks (Japan Clea), and male C57BL/6 mice and ApoE-KO mice on C57BL/6 background aged 4–6 weeks (Jackson Laboratory) were used in this study. All of the experimental protocols were approved by the Animal Research Committee of the Kyorin University School of Medicine.

2.2. H_2O_2-induced EC apoptosis in rats and in culture

EC apoptosis was induced by 5-min intra-arterial treatment of a rat carotid artery with 0.01 mmol/L H_2O_2 as previously described [23]. Briefly, edaravone (3-methyl-1-phenyl-2-pyrazolin-5-one; 3 or 10 mg/kg; donated by Mitsubishi Pharma Corporation, Japan) or its vehicle was intraperitoneally injected daily for 3 days before H_2O_2 treatment. A catheter was placed in the common carotid artery via the external carotid artery. The lumen was flushed with saline, replaced with 0.01 mmol/L H_2O_2 diluted with saline for 5 min and recovered. At 24 h after H_2O_2 treatment, EC apoptosis was evaluated by chromatin staining of *en face* specimens of the carotid artery using Hoechst 33342 dye. Apoptotic cells were identified by their typical morphological appearance; chromatin condensation, nuclear fragmentation, or apoptotic bodies. The numbers of apoptotic cells and intact cells were counted in 10 high-power fields for each specimen by an observer blinded to the treatment group.

Apoptosis of ECs isolated from a bovine carotid artery was induced as previously described [24]. Briefly, subconfluent ECs were pretreated for 24 h with culture medium containing edaravone or vehicle. After washing twice with Hank's balanced salt solution, the cells were exposed to H_2O_2 (0.2 mmol/L) diluted in Hank's balanced salt solution for 1.5 h at 37 °C to induce apoptosis. Then ECs were cultured in culture medium containing edaravone or vehicle until assay. Apoptosis was evaluated at 24 h after H_2O_2 treatment as histone-associated DNA fragments using a photometric enzyme immunoassay (Cell Death Detection ELISA, Roche), according to the manufacturer's instructions.

2.3. Atherosclerosis in ApoE-KO mice

ApoE-KO mice received a high-cholesterol diet (1% cholesterol, 10% fat in CE-2 standard diet; Japan Clea) for 4 weeks. Simultaneously, edaravone (10 mg/kg) or its vehicle was intra-peritoneally injected daily throughout the experiments. Body weight and systolic blood pressure were recorded every week in a conscious state by the tail cuff method (BP-98A; Softron, Tokyo).

At 4 weeks of treatment, mice were sacrificed with an overdose of diethyl ether and perfusion-fixed. Atherosclerotic lesions in the aortic sinus were quantified according to the method described previously [25]. We also measured the surface area of atherosclerotic lesions in the whole descending aorta including the abdominal aorta just proximal to the iliac bifurcation. *En face* specimens of the descending aorta were stained with oil red O, photographed and analyzed using the NIH image software. Total cholesterol, high-density lipoprotein cholesterol and low-density lipoprotein cholesterol in mice plasma were determined by a commercial laboratory (SRL, Japan).

2.4. Measurement of ROS

Aortic samples for ROS measurements were prepared separately from those for atherosclerosis evaluation. At 4 weeks of treatment, ApoE-KO mice were sacrificed with CO_2 inhalation. Descending aortas were rapidly removed and placed into chilled modified Krebs/HEPES buffer. C57BL/6 mice fed a standard diet were also used as the control. To determine superoxide production *in situ*, frozen cross-sections of the aorta were stained with 10 μmol/L dihydroethidium (DHE; Molecular Probes), followed by fluorescent microscopy [26]. Also, superoxide production in aortic rings was quantified using the superoxide dismutase-inhibitable cytochrome *c* reduction assay as previously described [27]. Immunohistochemical detection of 3-nitrotyrosine in the aorta was visualized by diaminobenzidine as reported previously [28].

Intracellular production of superoxide anions was measured using DHE as described previously [29], and the intensity values were calculated using the Metamorph software [24]. Concentrations of 8-isoprostane (8-iso prostaglandin

$F_{2\alpha}$) in the culture supernatants and mouse plasma were measured using a commercially available EIA kit (Cayman Chemical). Culture supernatants were directly applied to EIA, while plasma was applied to EIA after solid phase extraction purification according to the manufacturer's instructions.

2.5. Western blotting

Western blotting was performed as previously described [30], to detect the expression of VCAM-1 and 4-HNE in cultured ECs and mouse aortas. Descending aortas were prepared as described in ROS measurements. The antibodies used in this study were anti-4-HNE monoclonal antibody (JaICA, Shizuoka, Japan), anti-VCAM-1 polyclonal antibody (Santa Cruz Biotechnology) and anti-3-nitrotyrosine monoclonal antibody (Upstate). Densitometric analysis was performed using an image scanner and the NIH software.

2.6. Data analysis

All values are express as mean ± S.E.M. Data were analyzed using one-factor ANOVA. If a statistically significant effect was found, Newman–Keuls' test was performed to isolate the difference between the groups. Differences with a value of $P < 0.05$ were considered statistically significant.

3. Results

3.1. Effects of edaravone on H_2O_2-induced EC apoptosis and ROS

As shown in Fig. 1A, edaravone dose-dependently inhibited EC apoptosis in culture, which was induced 24 h after H_2O_2 treatment. Edaravone was then employed in a rat model of H_2O_2-induced EC apoptosis. Consistent with the *in vitro* experiment, edaravone of 10 mg/kg/day decreased EC apoptosis of the rat carotid artery by approximately 40% (Fig. 1B).

We next examined whether edaravone decreased ROS production in the process of H_2O_2-induced EC apoptosis. For this purpose, DHE fluorescent, a marker of intracellular production of superoxide anions, release of 8-isoprostane into the culture supernatants and accumulation of 4-HNE, a pivotal end-product of lipid peroxidation [31], were measured using cultured ECs. We also examined the expression of VCAM-1 as a marker of endothelial injury or activation [32]. Edaravone decreased DHE fluorescent, 8-isoprostane formation and VCAM-1 expression at 3 h after H_2O_2 treatment in a dose-dependent manner (Fig. 2A–C). As shown in Fig. 2D, multiple bands showing 4-HNE-Michael protein adducts [33,34] were accumulated after H_2O_2 treatment in a time-dependent manner. Consequently, the effect of edaravone on 4-HNE expression was examined at 3 h after H_2O_2 treatment (4.5 h after H_2O_2 was initially added). Edaravone decreased 4-HNE expression in a dose dependent manner.

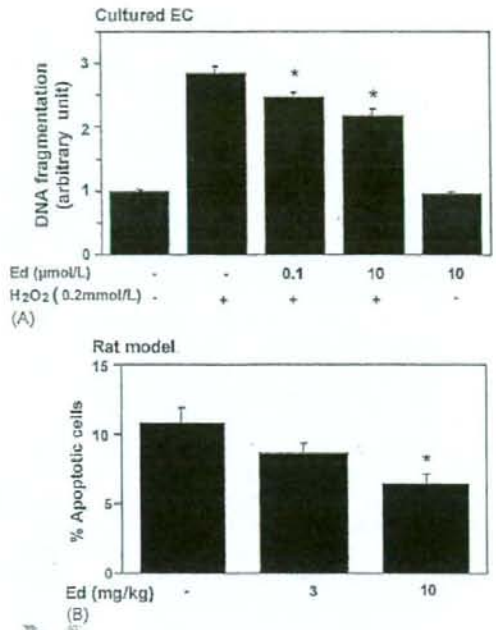

Fig. 1. Effects of edaravone (Ed) on H_2O_2-induced EC apoptosis in culture (A) and in a rat model (B). (A) Ed or its vehicle was added to the culture medium 24 h before H_2O_2 treatment until assay. EC apoptosis was evaluated 24 h after H_2O_2 treatment (0.2 mmol/L) by means of DNA fragmentation. Values are expressed as mean ± S.E.M. ($n = 3$). $^*P < 0.05$ vs. H_2O_2 (+) + Ed (−). (B) Ed or its vehicle was intraperitoneally injected once a day for 3 days before H_2O_2 treatment. At 24 h after H_2O_2 treatment, apoptotic ECs were counted per high power field and the ratio of the apoptotic cell number to the intact cells was calculated using *en face* specimens of the carotid artery stained with Hoechst 33342. Values are expressed as mean ± S.E.M. ($n = 7$). $^*P < 0.05$ vs. vehicle.

3.2. Effects of edaravone on atherosclerotic lesions and ROS in ApoE-KO mice

In the next set of experiments, we examined whether edaravone could suppress the atherosclerotic lesions in ApoE-KO mice fed a high cholesterol diet for 4 weeks. As shown in Fig. 3A and B, atheromatous lesions both in the aortic sinus and the descending aorta were smaller in mice treated with 10 mg/kg/day edaravone than in those with vehicle. This dose of edaravone did not influence body weight, blood pressure or plasma LDL and HDL cholesterol levels (Table 1).

Then, we examined whether the anti-atherogenic effects of edaravone were associated with the decrease in ROS production. Peroxynitrite formation was assessed as 3-nitrotyrosine accumulation in the aorta [28]. Both immunohistochemistry and Western blotting showed that edaravone inhibited nitrotyrosine accumulation in the aorta of ApoE-KO mice (Fig. 4A(a) and A(b)). Superoxide production *in situ* was examined using DHE staining of the descend-

Table 1
Body weight, blood pressure and plasma lipid levels in ApoE-KO mice treated with edaravone or vehicle

	Vehicle	Edaravone
Body weight (g)	21.4 ± 0.5	21.0 ± 0.5
Systolic blood pressure (mmHg)	106 ± 2	103 ± 3
Total cholesterol (mg/dL)	1967 ± 38	1872 ± 66
HDL cholesterol (mg/dL)	66 ± 6	82 ± 9
LDL cholesterol (mg/dL)	602 ± 24	602 ± 12

The values are shown as mean ± S.E. ($n = 14$). There were no significant differences in the values between the two groups.

ing aorta. As shown in Fig. 4B, ethidium fluorescence, which was amplified in ApoE-KO mice, was decreased by edaravone treatment. A quantitative analysis by the superoxide dismutase-inhibitable cytochrome *c* reduction assay revealed that $O_2^{\bullet -}$ levels in aortic rings of ApoE-KO mice were decreased by 43% in edaravone-treated ApoE-KO mice compared to those in vehicle-treated mice (Fig. 4C). Consistent with these results, plasma 8-isoprostane levels and 4-HNE expression in the descending aorta, both of which were elevated in ApoE-KO mice compared to

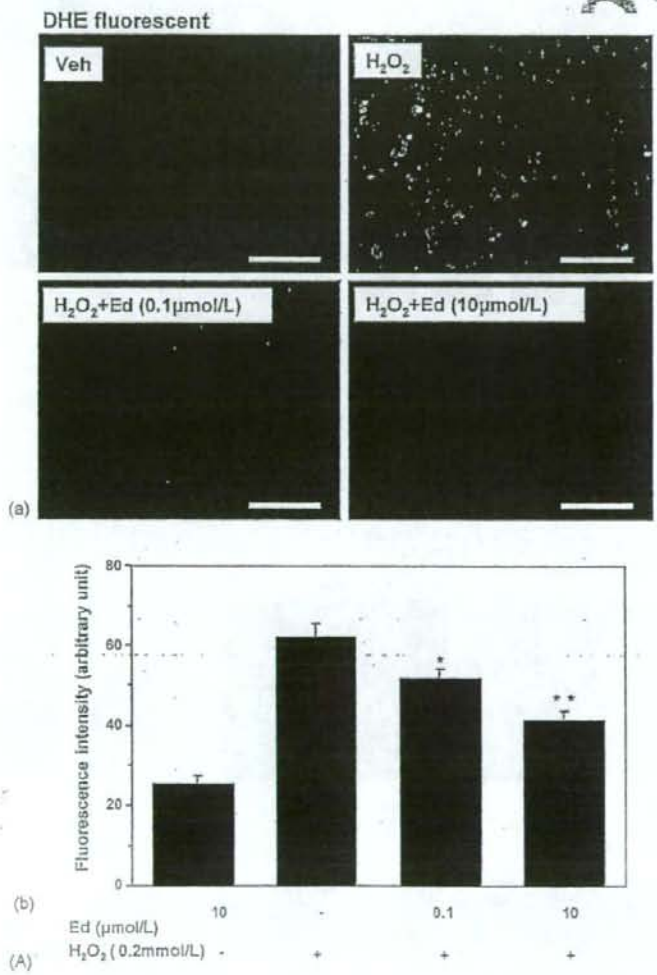

Fig. 2. Effects of edaravone (Ed) on DHE fluorescent (A) and 8-isoprostane formation (B), VCAM-1 expression (C) and 4-HNE expression (D) in cultured EC. Ed or its vehicle was added to the culture medium 24 h before H_2O_2 treatment until assay. DHE fluorescent ($n = 6$), 8-isoprostane concentration ($n = 3$) and VCAM-1 expression ($n = 3$) in the cell lysate were measured 3 h after H_2O_2 treatment. Values are expressed as mean ± S.E.M. Time dependent changes of 4-HNE expression after H_2O_2 treatment was detected by Western blotting. Representative image showed that 4-HNE-Michael protein adducts were accumulated after treatment (D(a)). The major 97 kDa band was measured 4.5 h after H_2O_2 treatment in the presence or absence of edaravone (D(b)). Values are expressed as mean ± S.E.M. ($n = 3$). $^{*}P < 0.05$, $^{**}P < 0.01$ vs. H_2O_2 (+) + Ed (−).

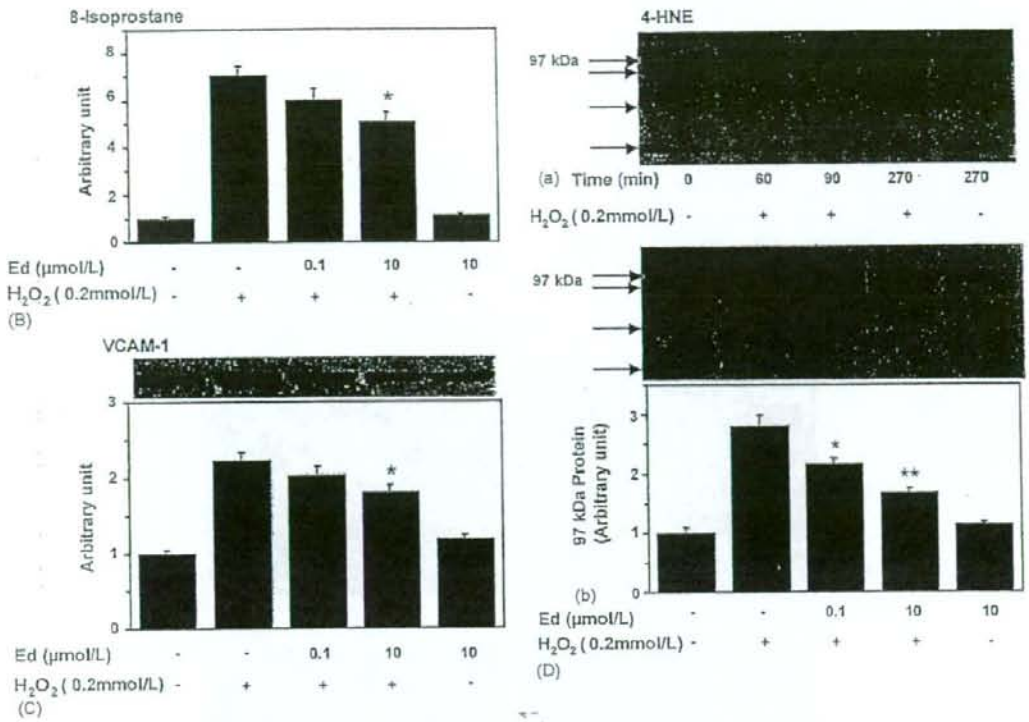

Fig. 2. (*Continued*).

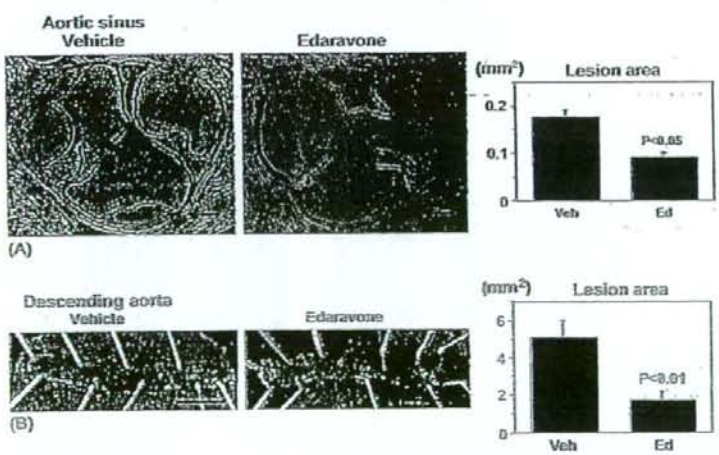

Fig. 3. Effects of edaravone on atherosclerotic lesion in ApoE-KO mice. ApoE-KO mice were fed a high-cholesterol diet for 4 weeks with the administration of edaravone (10 mg/kg daily) or its vehicle by i.p. injection. (A) Oil red O-stained cross-sections of the aortic sinus (bar = 100 μm) and morphometric analysis of the lesions are shown. (B) Oil red O-stained *en face* specimens of the descending aorta (bar = 5 mm) and morphometric analysis of the lesions are shown. Values are expressed as mean ± S.E.M. ($n = 14$).

those in wild-type C57BL/6 mice fed a normal chow, were decreased by edaravone treatment (Fig. 4D and E). Finally, the increase in VCAM-1 expression in the aorta of ApoE-KO mice was attenuated by edaravone as well (Fig. 4F).

4. Discussion

A number of studies have shown that ROS contribute to the pathogenesis of endothelial dysfunction and atherosclerosis formation. In addition to $O_2^{\bullet -}$ that is predominantly pro-

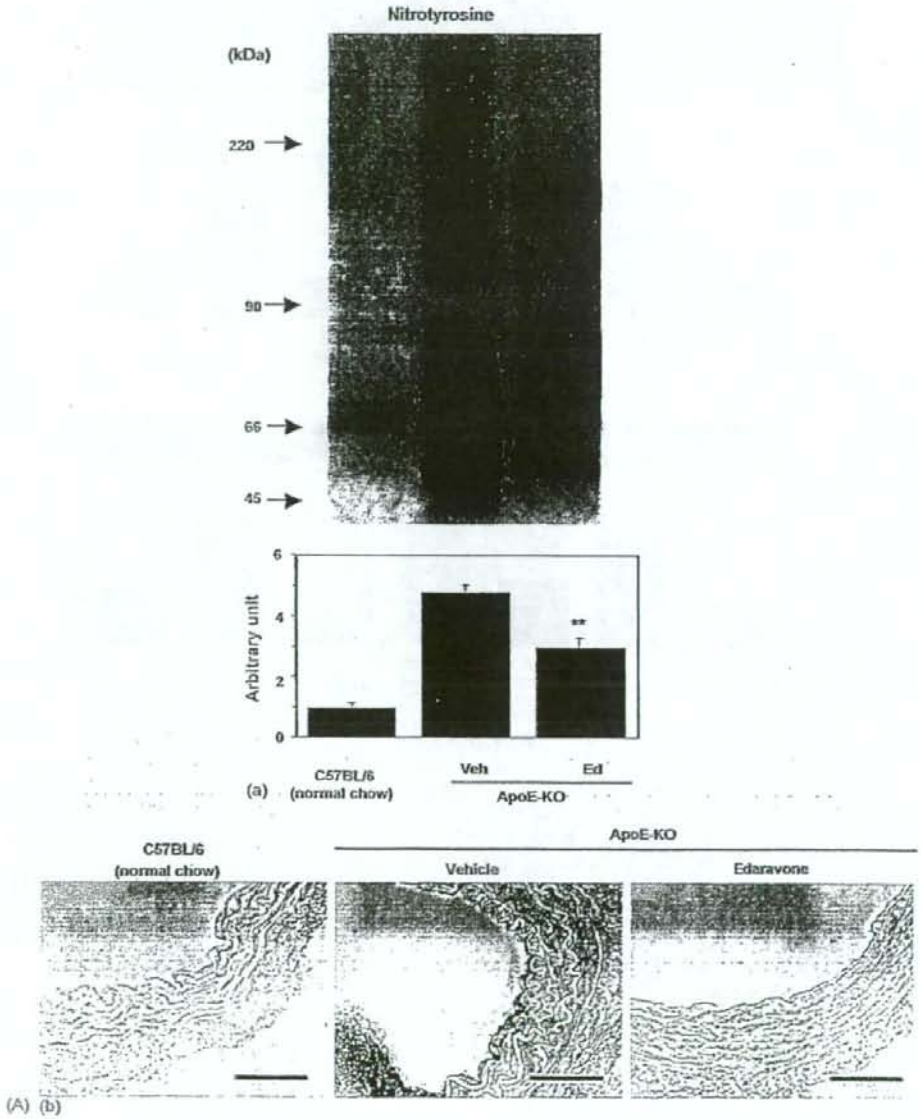

Fig. 4. Effects of edaravone (Ed) on ROS production (A–E) and VCAM-1 expression (F) in ApoE-KO mice. (A) Nitrotyrosine contents in the aorta was examined by Western blot analysis (A(a), $n=6$) and immunohistochemistry (A(b)). Bar = 50 μm. (B) Fresh-frozen cross-sections of the aorta were stained with DHE, and representative fluorescent micrographs are shown (bar = 100 μm). (C) Superoxide anion in aortic rings was determined using SOD inhibitable-cytochrome *c* reduction assay ($n=6$). (D) 8-Isoprostane level in mouse plasma was measured with EIA ($n=6$). (E and F) Representative Western blotting for 4-HNE (97 kDa band) and VCAM-1 expression in the aorta and densitometric analysis are shown ($n=3$). Values are expressed as mean ± S.E.M. $^{*}P<0.05$, $^{**}P<0.01$ vs. vehicle (Veh). C57/BL6 mice fed a normal chow serve as the control.

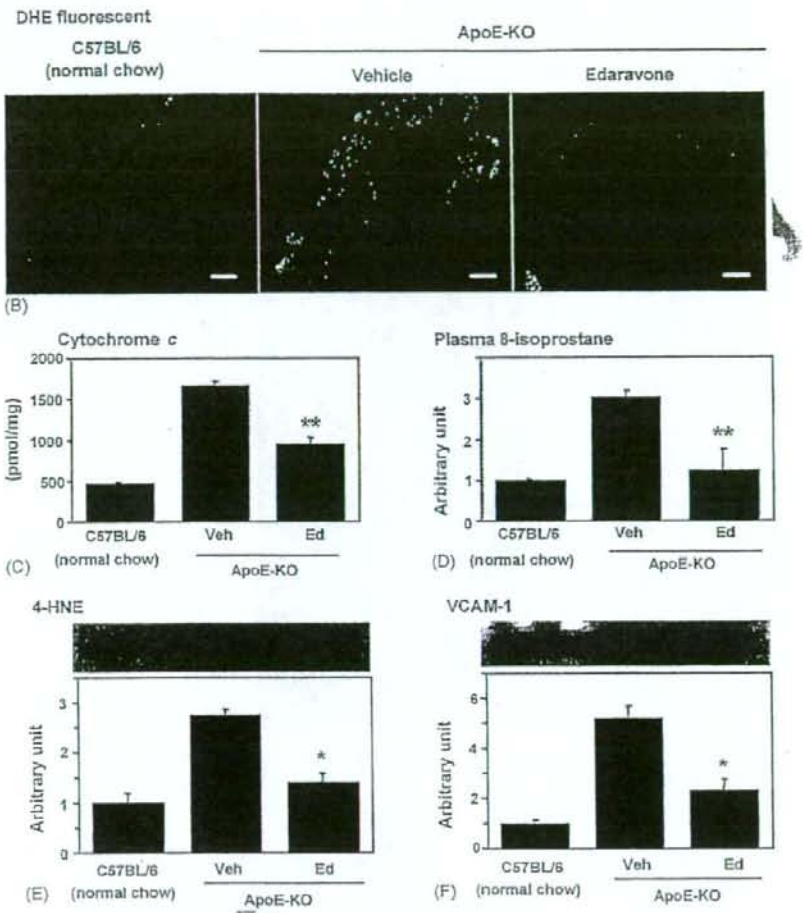

Fig. 4. (*Continued*).

duced via NAD(P)H oxidase [35], $^{\bullet}OH$ as well as $LOO^{\bullet}$ [36] and $ONOO^{-}$ [37] play a role in atherogenesis. In particular, $^{\bullet}OH$ is extremely strong in terms of oxidative activity and cellular damage [38]. Therefore, it might be essential to scavenge the wide range of ROS for the prevention of atherosclerosis. As a matter of fact, recent clinical trials have denied the protective effects of Vitamin E, which predominantly reacts with $LOO^{\bullet}$ [39], on cardiovascular events [18,19].

Edaravone, a potent free radical scavenger with unique properties, works by donating an electron from edaravone anion to free radicals [22]. Edaravone quenches $^{\bullet}OH$ and inhibits both $^{\bullet}OH$-dependent and $^{\bullet}OH$-independent lipid peroxidation [22]. Edaravone shows inhibitory effects on both water-soluble and lipid-soluble LOO-induced peroxidation systems [22]. Edaravone also inhibits $ONOO^{-}$-induced tyrosine nitration [22]. These properties are different from those of water-soluble Vitamin C and lipid-soluble Vitamin E.

In the present study, we demonstrated that edaravone suppressed endothelial apoptosis and fatty streak formation. Reduced expression of VCAM-1, a marker of vascular injury and activation [32], were corroborated with these results. In cultured ECs, protein expression of VCAM-1 was induced as early as 3 h after H_2O_2 treatment (actually 4.5 h after addition of H_2O_2, Fig. 2C). This is reasonable based on our time course experiments (data not shown), and is consistent with the previous reports that VCAM-1 protein has been induced 4–6 h after cytokine stimulation through an antioxidant-sensitive mechanism [40,41]. Although the experimental conditions were different between the cell culture and animal studies, edaravone inhibited both the rapid induction of VCAM-1 in cultured ECs and the chronic upregulation of VCAM-1 in the aorta of ApoE-KO mice, further supporting the vasoprotective effects of edaravone.

Edaravone has been clinically used as a neuroprotectant in the treatment of ischemic stroke in Japan from 2001. The dose of edaravone used in this study (intraperitoneal injection of 10 mg/kg) has been reported to be comparable to that of intravenous injection in clinical use in terms of plasma concentration [42]. This compound has been reported to preserve endothelial function in ischemic brain [43] and ameliorate ischemia-reperfusion injury in various organs such as kidney [44] and heart [45]. Also, edaravone has been shown to inhibit pressure overload-induced cardiac hypertrophy [42]. To our knowledge, however, the effect of edaravone on atherosclerosis has never been reported till now.

The effects of edaravone on endothelial injury and atherosclerosis were associated with the decrease in ROS production including peroxynitrite, superoxide anion and 8-isoprostane, suggesting the mechanistic role of antioxidation in vascular protection. Edaravone also inhibited the expression of 4-HNE in vascular tissues, further indicating the antioxidant activity and suggesting the signaling cascade leading to endothelial injury, because 4-HNE triggers cellular damages through the MAP kinase pathway as an end-product of ROS [34]. Antioxidant effects of edaravone on lipoproteins were not determined in the present study because of the methodological limitation in mice. It has been reported, however, that edaravone can inhibit oxidative modification of low-density lipoprotein *in vitro* and in rats [46]. Consequently, it is likely that reduced lipoprotein oxidation would have played a role in the anti-atherosclerotic effects of edaravone in ApoE-KO mice. Furthermore, edaravone has been reported to stimulate the expression of endothelial nitric oxide synthase in cultured ECs [46] and the artery [47], leading to the increased production of nitric oxide. Taken together with the effects on peroxynitrite formation, edaravone might synergistically increase the availability of nitric oxide, which exerts vasoprotective and anti-atherosclerotic action.

The effects of edaravone on advanced and complicated lesions of atherosclerosis were not investigated in this study. Neither, the effects on plaque ruptures nor consequent cardiovascular events are known. This study demonstrated that edaravone might be a potential new therapeutic agent for the prevention and treatment of early atherosclerosis. For the purpose of chronic use, however, the innovation of drug preparation for oral administration is necessary. Another application of edaravone might be the prevention of restenosis after percutaneous coronary interventions, since ROS plays an important role in neointimal formation after angioplasty [48]. Intravenous injection of edaravone for several days might inhibit neointimal formation in addition to ischemia reperfusion injury of cardiomyocytes [45]. Taken together, edaravone is expected to show protective effect on ROS-related vascular diseases beyond cerebral infarction.

In summary, edaravone, a free radical scavenger with unique properties, attenuated oxidative stress-induced endothelial damage in rats and early atherosclerosis in ApoE-KO mice in association with the inhibition of ROS formation. These findings provide new information on the role of ROS in atherogenesis and the therapeutic strategy for atherosclerosis.

Acknowledgements

We thank Ms. Mariko Sawano for her excellent technical assistance. This study was supported by a Grant-in-Aid for Scientific Research from the Ministry of Education, Science, Culture and Sports of Japan (13670741), and by Health and Labour Sciences Research Grants (H15-Choju-013, H15-Choju-015 and H17-Choju-046) from the Ministry of Health, Labour and Welfare of Japan.

References

[1] Ross R. Atherosclerosis—an inflammatory disease. N Engl J Med 1999;340:115–26.
[2] Griendling KK, Sorescu D, Lassegue B, Ushio-Fukai M. Modulation of protein kinase activity and gene expression by reactive oxygen species and their role in vascular physiology and pathophysiology. Arterioscler Thromb Vasc Biol 2000;20:2175–83.
[3] Zalba G, San Jose G, Moreno MU, et al. Oxidative stress in arterial hypertension: role of NAD(P)H oxidase. Hypertension 2001;38:1395–9.
[4] Sorescu D, Weiss D, Lassegue B, et al. Superoxide production and expression of nox family proteins in human atherosclerosis. Circulation 2002;105:1429–35.
[5] Spiekermann S, Landmesser U, Dikalov S, et al. Electron spin resonance characterization of vascular xanthine and NAD(P)H oxidase activity in patients with coronary artery disease: relation to endothelium-dependent vasodilation. Circulation 2003;107:1383–9.
[6] Rey FE, Li XC, Carretero OA, Garvin JL, Pagano PJ. Perivascular superoxide anion contributes to impairment of endothelium-dependent relaxation: role of gp91(phox). Circulation 2002;106:2497–502.
[7] Barry-Lane PA, Patterson C, van der Merwe M, et al. p47phox is required for atherosclerotic lesion progression in ApoE(−/−) mice. J Clin Invest 2001;108:1513–22.
[8] Keaney Jr JF, Gaziano JM, Xu A, et al. Dietary antioxidants preserve endothelium-dependent vessel relaxation in cholesterol-fed rabbits. Proc Natl Acad Sci (USA) 1993;90:11880–4.
[9] Keaney Jr JF, Xu A, Cunningham D, Jackson T, Frei B, Vita JA. Dietary probucol preserves endothelial function in cholesterol-fed rabbits by limiting vascular oxidative stress and superoxide generation. J Clin Invest 1995;95:2520–9.
[10] Lamb DJ, Reeves GL, Taylor A, Ferns GA. Dietary copper supplementation reduces atherosclerosis in the cholesterol-fed rabbit. Atherosclerosis 1999;146:33–43.
[11] Pratico D, Tangirala RK, Rader DJ, Rokach J, FitzGerald GA. Vitamin E suppresses isoprostane generation in vivo and reduces atherosclerosis in ApoE-deficient mice. Nat Med 1998;4:1189–92.
[12] Li Z, Iwai M, Wu L, et al. Fluvastatin enhances the inhibitory effects of a selective AT1 receptor blocker, valsartan, on atherosclerosis. Hypertension 2004;44:758–63.
[13] Fennell JP, Brosnan MJ, Frater AJ, et al. Adenovirus-mediated overexpression of extracellular superoxide dismutase improves endothelial dysfunction in a rat model of hypertension. Gene Ther 2002;9:110–7.
[14] Kirk EA, Dinauer MC, Rosen H, Chait A, Heinecke JW, LeBoeuf RC. Impaired superoxide production due to a deficiency in phagocyte NADPH oxidase fails to inhibit atherosclerosis in mice. Arterioscler Thromb Vasc Biol 2000;20:1529–35.

[15] Hsich E, Segal BH, Pagano PJ, et al. Vascular effects following homozygous disruption of p47(phox): an essential component of NADPH oxidase. Circulation 2000;101:1234–6.
[16] Fang JC, Kinlay S, Beltrame J, et al. Effect of Vitamins C and E on progression of transplant-associated arteriosclerosis: a randomised trial. Lancet 2002;359:1108–13.
[17] Engler MM, Engler MB, Malloy MJ, et al. Antioxidant Vitamins C and E improve endothelial function in children with hyperlipidemia: endothelial assessment of risk from lipids in youth (EARLY) trial. Circulation 2003;108:1059–63.
[18] Lonn E, Bosch J, Yusuf S, et al. Effects of long-term Vitamin E supplementation on cardiovascular events and cancer: a randomized controlled trial. JAMA 2005;293:1338–47.
[19] Lee IM, Cook NR, Gaziano JM, et al. Vitamin E in the primary prevention of cardiovascular disease and cancer: the Women's Health Study: a randomized controlled trial. JAMA 2005;294:56–65.
[20] Study-Group E. Effect of a novel free radical scavenger, edaravone (MCI-186), on acute brain infarction. Randomized, placebo-controlled, double-blind study at multicenters. Cerebrovasc Dis 2003;15:222–9.
[21] Abe S, Kirima K, Tsuchiya K, et al. The reaction rate of edaravone (3-methyl-1-phenyl-2-pyrazolin-5-one (MCI-186)) with hydroxyl radical. Chem Pharm Bull (Tokyo) 2004;52:186–91.
[22] Watanabe T, Yuki S, Egawa M, Nishi H. Protective effects of MCI-186 on cerebral ischemia: possible involvement of free radical scavenging and antioxidant actions. J Pharmacol Exp Ther 1994;268:1597–604.
[23] Sudoh N, Toba K, Akishita M, et al. Estrogen prevents oxidative stress-induced endothelial cell apoptosis in rata. Circulation 2001;103:724–9.
[24] Akishita M, Nagai K, Xi H, et al. Renin–angiotensin system modulates oxidative stress-induced endothelial cell apoptosis in rats. Hypertension 2005;45:1188–93.
[25] Paigen B, Morrow A, Holmes PA, Mitchell D, Williams RA. Quantitative assessment of atherosclerotic lesions in mice. Atherosclerosis 1987;68:231–40.
[26] Miller Jr FJ, Gutterman DD, Rios CD, Heistad DD, Davidson BL. Superoxide production in vascular smooth muscle contributes to oxidative stress and impaired relaxation in atherosclerosis. Circ Res 1998;82:1298–305.
[27] Landmesser U, Dikalov S, Price SR, et al. Oxidation of tetrahydrobiopterin leads to uncoupling of endothelial cell nitric oxide synthase in hypertension. J Clin Invest 2003;111:1201–9.
[28] Francia P, Delli Gatti C, Bachschmid M, et al. Deletion of p66shc gene protects against age-related endothelial dysfunction. Circulation 2004;110:2889–95.
[29] Carter WO, Narayanan PK, Robinson JP. Intracellular hydrogen peroxide and superoxide anion detection in endothelial cells. J Leuk Biol 1994;55:253–8.
[30] Xi H, Shin WS, Suzuki J, et al. Dystrophin disruption might be related to myocardial cell apoptosis caused by isoproterenol. J Cardiovasc Pharmacol 2000;36(Suppl 2):S25–9.
[31] Esterbauer H, Schaur RJ, Zollner H. Chemistry and biochemistry of 4-hydroxynonenal, malonaldehyde and related aldehydes. Free Radic Biol Med 1991;11:81–128.
[32] Meigs JB, Hu FB, Rifai N, Manson JE. Biomarkers of endothelial dysfunction and risk of type 2 diabetes mellitus. JAMA 2004;291:1978–86.
[33] Uchida K, Toyokuni S, Nishikawa K, et al. Michael addition-type 4-hydroxy-2-nonenal adducts in modified low-density lipoproteins: markers for atherosclerosis. Biochemistry 1994;33:12487–94.
[34] Usatyuk PV, Natarajan V. Role of mitogen-activated protein kinases in 4-hydroxy-2-nonenal-induced actin remodeling and barrier function in endothelial cells. J Biol Chem 2004;279:11789–97.
[35] Jiang F, Guo Y, Salvemini D, Dusting GJ. Superoxide dismutase mimetic M40403 improves endothelial function in apolipoprotein (E)-deficient mice. Br J Pharmacol 2003;139:1127–34.
[36] O'Donnell VB, Chumley PH, Hogg N, Bloodsworth A, Darley-Usmar VM, Freeman BA. Nitric oxide inhibition of lipid peroxidation: kinetics of reaction with lipid peroxyl radicals and comparison with alpha-tocopherol. Biochemistry 1997;36:15216–23.
[37] White CR, Brock TA, Chang LY, et al. Superoxide and peroxynitrite in atherosclerosis. Proc Natl Acad Sci USA 1994;91:1044–8.
[38] Zheng H, Dimayuga C, Hudaihed A, Katz SD. Effect of dexrazoxane on homocysteine-induced endothelial dysfunction in normal subjects. Arterioscler Thromb Vasc Biol 2002;22:E15–8.
[39] Terentis AC, Thomas SR, Burr JA, Liebler DC, Stocker R. Vitamin E oxidation in human atherosclerotic lesions. Circ Res 2002;90:333–9.
[40] Marui N, Offermann MK, Swerlick R, et al. Vascular cell adhesion molecule-1 (VCAM-1) gene transcription and expression are regulated through an antioxidant-sensitive mechanism in human vascular endothelial cells. J Clin Invest 1993;92:1866–74.
[41] Park SH, Park JH, Kang JS, Kang YH. Involvement of transcription factors in plasma HDL protection against TNF-alpha-induced vascular cell adhesion molecule-1 expression. Int J Biochem Cell Biol 2003;35:168–82.
[42] Tsujimoto I, Hikoso S, Yamaguchi O, et al. The antioxidant edaravone attenuates pressure overload-induced left ventricular hypertrophy. Hypertension 2005;45:921–6.
[43] Amemiya S, Kamiya T, Nito C, et al. Anti-apoptotic and neuroprotective effects of edaravone following transient focal ischemia in rats. Eur J Pharmacol 2005;516:125–30.
[44] Doi K, Suzuki Y, Nakao A, Fujita T, Noiri E. Radical scavenger edaravone developed for clinical use ameliorates ischemia/reperfusion injury in rat kidney. Kidney Int 2004;65:1714–23.
[45] Tsujita K, Shimomura H, Kawano H, et al. Effects of edaravone on reperfusion injury in patients with acute myocardial infarction. Am J Cardiol 2004;94:481–4.
[46] Yoshida H, Sasaki K, Namiki Y, Sato N, Edaravone TN. a novel radical scavenger, inhibits oxidative modification of low-density lipoprotein (LDL) and reverses oxidized LDL-mediated reduction in the expression of endothelial nitric oxide synthase. Atherosclerosis 2005;179:97–102.
[47] Zhang XH, Matsuda N, Jesmin S, et al. Normalization by edaravone, a free radical scavenger, of irradiation-reduced endothelial nitric oxide synthase expression. Eur J Pharmacol 2003;476:131–7.
[48] Cipollone F, Fazia M, Iezzi A, et al. High preprocedural non-HDL cholesterol is associated with enhanced oxidative stress and monocyte activation after coronary angioplasty: possible implications in restenosis. Heart 2003;89:773–9.

Available online at www.sciencedirect.com
ScienceDirect
European Journal of Pharmacology 556 (2007) 1–8
ejp
www.elsevier.com/locate/ejphar

Gas6/Axl-PI3K/Akt pathway plays a central role in the effect of statins on inorganic phosphate-induced calcification of vascular smooth muscle cells

Bo-Kyung Son [a], Koichi Kozaki [b], Katsuya Iijima [a], Masato Eto [a], Toru Nakano [c], Masahiro Akishita [a], Yasuyoshi Ouchi [a,*]

[a] *Department of Geriatric Medicine, Graduate School of Medicine, The University of Tokyo, 7-3-1 Hongo, Bunkyo-ku, Tokyo 113-8655, Japan*
[b] *Department of Geriatric Medicine, Kyorin University School of Medicine, Tokyo, Japan*
[c] *Discovery Research Laboratory, Shionogi and Co., Ltd., Osaka, Japan*

Received 19 May 2006; received in revised form 22 September 2006; accepted 27 September 2006
Available online 18 October 2006

Abstract

Apoptosis is essential for the initiation and progression of vascular calcification. Recently, we showed that *3-hydroxy-3-methylglutaryl* (HMG) CoA reductase inhibitors (statins) have a protective effect against vascular smooth muscle cell calcification by inhibiting apoptosis, where growth arrest-specific gene 6 (Gas6) plays a pivotal role. In the present study, we clarified the downstream targets of Gas6-mediated survival signaling in inorganic phosphate (Pi)-induced apoptosis and examined the effect of statins. We found that fluvastatin and pravastatin significantly inhibited Pi-induced apoptosis and calcification in a concentration-dependent manner in human aortic smooth muscle cells (HASMC), as was found with atorvastatin previously. Gas6 and its receptor, Axl, expression were downregulated in the presence of Pi, and recombinant human Gas6 (rhGas6) significantly inhibited apoptosis and calcification in a concentration-dependent manner. During apoptosis, Pi suppressed Akt phosphorylation, which was reversed by rhGas6. Wortmannin, a specific *phosphatidylinositol 3-OH kinase* (PI3K) inhibitor, abolished the increase in Akt phosphorylation by rhGas6 and eliminated the inhibitory effect of rhGas6 on both Pi-induced apoptosis and calcification, suggesting that PI3K-Akt is a downstream signal of the Gas6-mediated survival pathway. Pi reduced phosphorylation of Bcl2 and Bad, and activated caspase 3, all of which were reversed by rhGas6. The inhibitory effect of statins on Pi-induced apoptosis was accompanied by restoration of the Gas6-mediated survival signal pathway: upregulation of Gas6 and Axl expression, increased phosphorylation of Akt and Bcl2, and inhibition of Bad and caspase 3 activation. These findings indicate that the Gas6-mediated survival pathway is the target of statins' effect to prevent vascular calcification.

Keywords: Calcification; Apoptosis; Gas6; Axl; Akt; Bcl2

1. Introduction

Vascular calcification, such as coronary and aortic calcification, is clinically important in the development of cardiovascular disease (Eggen, 1968). Two distinct forms of vascular calcification are well recognized. One is medial calcification, which occurs between the cell layers of smooth muscle cells and is related to aging, diabetes and chronic renal failure (Neubauer, 1971; Goodman et al., 2000). The other is atherosclerotic calcification, which occurs in the intima during the development of atheromatous disease (Wexler et al., 1996). In diabetic patients, medial calcification has been shown to be a strong independent predictor of cardiovascular mortality (Everhart et al., 1988).

We recently demonstrated that atorvastatin prevented inorganic phosphate (Pi)-induced calcification by inhibiting apoptosis, one of the important processes regulating calcification. This was mediated by growth arrest-specific gene 6 (Gas6), a vitamin K-dependent protein (Son et al., 2006). Gas6 binds to Axl, the predominant receptor for Gas6, on the cell surface and transduces the signal by Axl autophosphorylation (Mark et al., 1996). Gas6-Axl interaction has been shown to be implicated in the regulation of multiple cellular functions (Yanagita et al., 2001; Goruppi et al., 1996; Nakano et al., 1997; Fridell et al., 1998). Especially, they are known to protect a range of cell types

* Corresponding author. Tel.: +81 3 5800 8652; fax: +81 3 5800 6530.
E-mail address: youchi-tky@umin.ac.jp (Y. Ouchi).

0014-2999/$ - see front matter © 2006 Elsevier B.V. All rights reserved.
doi:10.1016/j.ejphar.2006.09.070